Available online at www.sciencedirect.com
SCIENCE DIRECT®
International Journal of Heat and Mass Transfer 49 (2006) 3942–3956
International Journal of HEAT and MASS TRANSFER
www.elsevier.com/locate/ijhmt

Mixing of confined coaxial flows

Valery Zhdanov [a,*], Nikolay Kornev [a], Egon Hassel [a], Andrei Chorny [b]

[a] Department of Technical Thermodynamics, University of Rostock, Rostock 18059, Germany
[b] Turbulence Laboratory, A.V. Luikov Heat and Mass Transfer Institute, 15, P. Brovka Str., Minsk 220072, Belarus

Received 17 April 2006
Available online 7 July 2006

Abstract

The paper presents experimental results on the mixing process in a coaxial jet mixer in two mixing regimes. In the first mixing regime, a recirculation zone develops just behind a nozzle near mixer walls, while in the second regime a jet is mixed with the co-flow without developing a recirculation zone. In the both regimes, the mixing process is studied at $Re_d = 10000$. Behind the nozzle over the range $0.1 < x/D < 9.1$, a velocity field in mixer cross-sections is measured by a one-component laser Doppler velocity meter and a scalar field is detected by the laser image fluorescence (LIF) method. A transverse autocorrelation function, integral length scales and probability density functions (PDF) are calculated using instantaneous distributions of a scalar and its fluctuations. It is shown that the scalar field acquires a homogeneous state faster than the velocity one. A quasi-uniform scalar distribution over the mixer cross-section is completed at the distance $x/D = 5.1$ in the first mixing regime, while this distribution has not been yet attained in the second. Analysis of the turbulent statistical moments and the autocorrelation function reveals how unsteady vortex structures exert a dramatic influence on the mixing. When the recirculation zone has developed, long-period antiphase oscillations exist near the mixer walls.

1. Introduction

Currently, studies of the mixing in confined coaxial jets have received considerable attention because the jet interaction causes a great number of physical phenomena to appear. Among them is the intermittence at the boundaries of mixing layers that originates due to generation, coalescence, and decay of unsteady vortex structures. In addition, entraining one flow by another can generate a prerequisite to the formation of separated flow regions. These phenomena are the objects of investigation which are of interest from the standpoint of both a deeper insight into transfer processes and finding of optimal mixing conditions in jet mixers.

The elaboration of experimental methods for measurement of passive admixture distributions has gained a notable advance in the understanding of the mixing process. The results on a scalar field developed under the action of a velocity one will essentially refine the understanding not only of the velocity evolution, but also of unsteady flow peculiarities that do not always emerge from velocity field experiments.

Coaxial jet mixers being rather simple engineering facilities find widespread use in different branches of industry and permit realizing the mixing process when the conditions for combination of laminar and turbulent flows are regulated through their flowrate ratio. There are a lot of possible mixing regimes. Some of these regimes were already detailed in the investigations of Rehalb [1,2] and Lima [3]. In these investigations, the mixing process was studied at the velocity of the co-flow much larger than that of the jet, in which a laminar flow was realized. At this condition, the recirculation zone developed just behind the nozzle along the mixer axis. These investigations were motivated by two following problems that had arisen in the study of chemically reacting flows: the stabilization of the flame front and the filling of the co-flow with substances transported by an internal jet.

The mixing with a jet velocity much higher than a co-flow one is less well understood. Under this condition,

* Corresponding author.
E-mail address: valery.zhdanov@uni-rostock.de (V. Zhdanov).

0017-9310/$ - see front matter © 2006 Elsevier Ltd. All rights reserved.
doi:10.1016/j.ijheatmasstransfer.2006.04.022

two fundamentally different mixing regimes can be generated. These regimes depend on the mixer geometry and the flowrate ratio of a considered medium.

When condition (1) $D/d > G + \dot{V}_D/\dot{V}_d$ is valid, there appears the mixing regime with a recirculation zone that develops just behind the nozzle near the mixer walls. Here D and d are the inner diameters of a mixer and a nozzle, respectively, $\dot{V}_D$ and $\dot{V}_d$ are the volume flowrates, $G \approx 1$ at equal densities of media being mixed [4]. For convenience, hereinafter, this regime will be called the r-mode regime and the ratio $\dot{V}_D/\dot{V}_d$ will be designated by Q. The r-mode regime involving multiple interactions between initial components and a mixed medium excludes its application in chemical reactors with competitive chemical reactions [5]. In such reactors, it is important to avoid undesirable competitive reactions since reaction products can interact with initial substances, thus decreasing the yield of desired product. For this not to occur, condition (2) $D/d < G + Q$ must hold true, when the jet and the co-flow are mixed, not forming a recirculation zone. This mixing regime will be called the j-mode regime.

Barchilon and Curtet [6] were the first who detailed an averaged velocity field in the mixing regime with the recirculation zone. They established a profound influence of the flowrate ratio on the spreading of such a zone. When the ratio Q was increased, the front boundary and the center of this zone displaced downstream, but the boundary of its decay was invariable and was at the distance $x/D \sim 3$ from the nozzle. Barchilon and Curtet [6] measured the averaged velocity using a Prandtl tube and registered velocity fluctuations by a hot-wire anemometer only at the mixer axis. So, taking into account a high level of turbulence (~40%), we can perform only a qualitative analysis of their behaviour. The flow visualization with an exposure time of 120 s showed that the jet deflects from its symmetry axis when it interacts with the recirculation zone full of a great number of vortices, whose size and position essentially vary with time. However, Barchilon and Curtet [6] had no proper equipment to estimate the influence of the fluid unsteadiness on mean flow characteristics and interpreted the recirculation zone as a three-dimensional steady symmetric vortex developing around the jet. Such a mixing model fully ignores the observed unsteady phenomena.

As shown [7], the development of velocity and scalar fields in the coaxial jet mixer within the r-mode regime does not depend on the Reynolds number over a broad range $40\,000 < Re_d = U_d d/\nu < 126\,000$. From the presented data on the development of velocity and scalar fields, it is difficult to get much information about the interaction of these fields in the flow field where the recirculation zone should develop. It seems that the authors [7] did not notice the formation of the recirculation zone, but they stated that the macromixing was completed already at $x/D \sim 3$. One of the reasons that hid the existence of the recirculation zone from the authors [7] is the fact that the changes in velocity and scalar distributions were diagnosed over the mixer cross-section only up to the distance $r/D = 0.4$. As shown [6], the backflow is registered near the mixer walls ($r/D > 0.45$) and so cannot be measured by the laser Doppler (LDV) technique [7]. However, the size of the investigated flow region in the mixer is quite enough to determine scalar changes due to flow dynamics. These changes were clearly observed in the works [8,9] on the mixing in the mixer with the same geometrical parameters and flowrate ratio. It was also noticed [8] that the mixing was not influenced by the temperature factor $(T_D - T_d)/T_D$.

Mortensen et al. [10] considered the j-mode mixing regime when a laminar jet issued from the nozzle. Only the decay of a scalar and its fluctuations along the mixer axis was registered. Studies were made at the Reynolds numbers $Re_D = 18\,500$–$66\,000$. It was shown that as the Reynolds number was increased, the starting length of the jet with a constant passive admixture concentration decreased about twice. A maximum recorded scalar fluctuation over the cross-section at $x/D \sim 1.0$ ($Re_D = 18\,500$) appeared at $x/D \sim 0.15$ when the Reynolds number was increased ($Re_D = 66\,000$). Investigations of jet mixers as chemical reactors were also made by Baldyga [11].

The above analysis of the investigations of mixing in coaxial jet mixers shows that there is a lack of simultaneous measurements of velocity and scalar fields in the r- and j-mode mixing regimes that are considered in this article. In Section 2, an experimental set-up is described. Averaged and fluctuation characteristics of velocity and scalar fields within the r- and j-mode mixing regimes are discussed in Section 3.1. An autocorrelation function and an integral length scale of scalar fluctuations are analyzed in Section 3.2. A structure of a recirculation zone is studied in Section 3.3. In addition to the common mixing characteristics, Section 3.4 is devoted to the study of a scalar probability density function (PDF) and the accuracy estimation of the PDF in the form of the β-distribution for different flow regimes. Distributions of the third and fourth turbulent statistical moments (Sk, T) are used to estimate whether the micromixing state has been reached in the flow.

2. Experimental set-up and measurement procedure

Experiment was made in a water closed-circuit channel [8,9]. Fig. 1 shows the design scheme of the mixer formed by two coaxial tubes: plexiglas tube 1 ($D = 50$ mm) and steel nozzle 2 with the inner diameter $d = 10$ mm. Nozzle 2 was fixed in detachable block 3 with length 430 mm. Tube 4 of 50 mm inner diameter had a movable joint with the flanges of block 3 via circular seals. Owing to this, the angular position, ϑ, of nozzle 2 relative to tube 1 could be varied by rotating tube 4 relative to fixed tube 1. This was done for investigation of flow axial asymmetry (see Section 3.1). Nozzle 2 was coaxially positioned along tube 4 with an accuracy of ± 0.3 mm. The mounting of block 3 provided tubes 1 and 4 to be coaxial not worse than ± 0.3 mm. The length of nozzle 2 was 550 mm, and its projection behind the plane of the outlet cross-section of tube 4 was 120 mm. The mixer was placed into rectangular

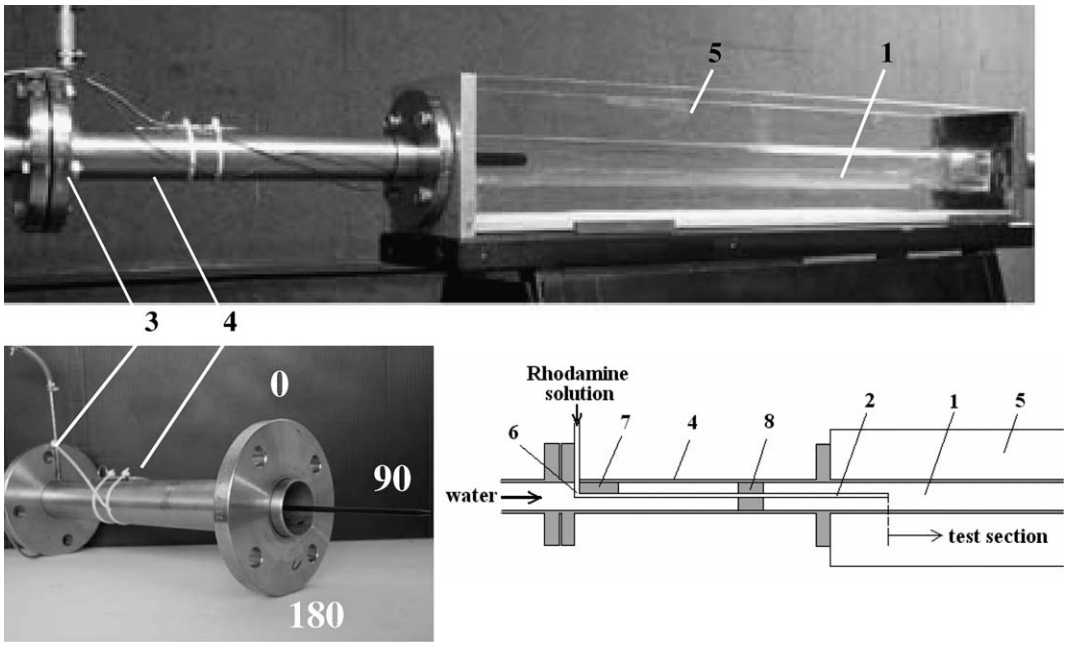

Fig. 1. Test section: 1 – mixer outer tube; 2 – nozzle; 3 – detachable block with nozzle 2; 4 – outer tube of block 3; 5 – water box; 6 – knee bend of nozzle 2; 7 – plate for damping of vortices shed from knee bend 6; 8 – support plates.

plexiglas box 5 filled with water to reduce undesirable optical distortions thank to the curvature of tube 1.

A velocity field was measured by a one-component laser Doppler anemometer (Flow Light 1, Firm Dantec Dynamics). Profiles of an averaged velocity and velocity fluctuations were registered in the mixer cross-sections, beginning with a distance of 1 mm from the nozzle outlet cross-section up to 9 mixer diameters downstream at three angular positions of the nozzle ($\vartheta = 0°$, 90°, and 180°).

A scalar field was measured by the LIF method. An aqueous solution of Rhodamine 6G with a concentration of 0.03 mg/L ejected from the nozzle was used as fluorescing substance. A measuring system comprised a Nd:YAG laser operating at a wavelength of 532 nm and with a pulse duration of 7 ns, a CCD camera (PI-MAX, Roper Sci. Corp) with a Nikkor 50 mm lens, and an optical unit to make a laser sheet [8]. The use of a ring Nikkor PK-11A between the CCD camera and the Nikkor lens enables increasing a spatial resolution up to 0.3 mm. The latter has been fixed by the number of pixels describing light intensity variation from zero to unity. The laser sheet was formed in the vertical plane along the mixer axis, and its thickness across the mixer did not exceed 0.5 ± 0.03 mm.

The CCD camera detected the instantaneous radiation intensity of mixture across the mixer diameter in the plane of the laser sheet 1 pixel wide (the so-called ROI option). Unlike the earlier study [8], the number of pixels that could fix fluorescence radiation across the mixer was increased four times, and the rate of data transmission from the CCD camera to a computer was increased by the order of magnitude and was limited only by the 10 Hz frequency of the laser used as an external trigger of the camera. For each considered mixer cross-section, a file contained 1000 instantaneous distributions corresponding to a measuring time of 100 s. A threefold time increase resulted in 1–2% variations of averaged and fluctuation characteristics of the scalar and yielded a 5% change in scalar PDF values. The location of the camera relative to the laser sheet was the same for all the measured mixer cross-sections. Calibration was made in the test section by replacing tube 1 by a calibration vessel of the same size. The vessel was filled with a mixture of given concentration. When calibrating, the laser sheet parameters were identical to the ones used in mixer measurements. From the calibration curves, the concentration range was determined, yielding a linear dependence between the concentration variation and applied laser power [8]. Also, correction curve was design, allowing one to eliminate CCD camera errors causing the measured radiation intensities to decrease in the mixer wall direction. This curve is used to correct the distribution of the emitted light intensity across the mixer. Scalar field variations in the mixer cross-section are estimated by varying one conservative scalar, namely, the "mixture fraction" f. It equals the ratio of the locally measured radiation intensity of fluorescing substance to its maximum value at the jet axis in the mixer cross-section at $x/D = 0.1$. The scalar decay along the axis downstream is determined as the ratio of the averaged mixture fraction at the current distance to the one at $x/D = 0.1$.

The development of velocity and scalar fields was studied at the flowrate ratios that provided the r-mode regime ($Q = 1.3$) and the j-mode one ($Q = 5$). In all cases, the nozzle jet was turbulent at the Reynolds number Re_d equal to 10 000.

3. Results

3.1. Averaged and root-mean-square characteristics of velocity and scalar fields

r-mode mixing regime. The velocity field near the mixer wall cannot be diagnosed because of the LDV signal instability due to the mixer wall curvature. So, LDV measurements ended at a distance of about 4 mm in front of the wall. Therefore, the averaged velocity profiles hardly fixed the backflow when the recirculation zone developed in the mixer.

Fig. 2 plots the velocity and scalar distributions measured in three different planes made by rotating nozzle 2 about the axis from $\vartheta = 0°$ to 180° with a step of 90°. They point to the flow axial asymmetry.

As mentioned previously, the accuracy of installing nozzle 2 into tube 4 was ±0.3 mm. So, a maximal transverse deviation along the length of nozzle 2 (550 mm) is around 1 mm. That deviation brings the maximal one (about ±0.1°) of nozzle 2. The flow disturbances caused by nozzle knee 6 and support plates 8 decayed to the nozzle exit because of the installation of plate 7 behind knee 6 and an additional small 0.5 mm thick support plate. Plate 7 forces the strong vortices generated by the tube knee to decay fast [12].

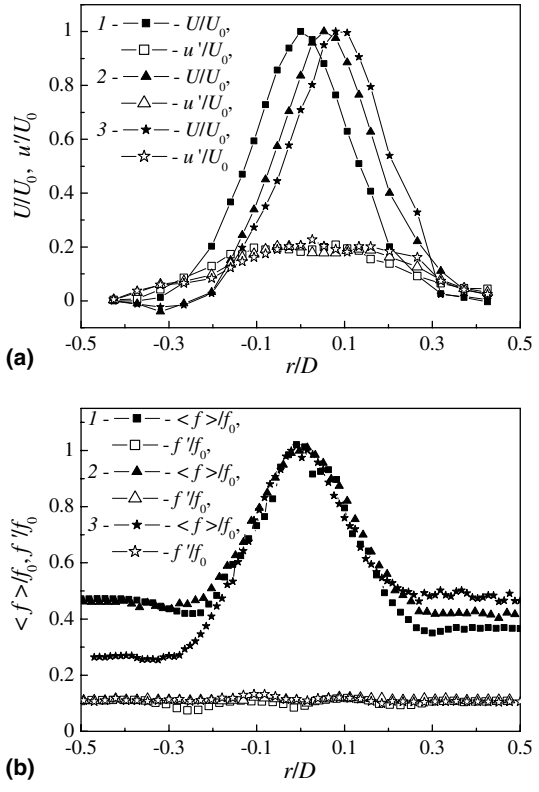

Fig. 2. Distributions of averaged velocity, scalar (closed symbols) and their root-mean-square fluctuations (open symbols) for $x/D = 1.6$ at three angular positions, υ, of nozzle 2 (see Fig. 1) for $Re_d = 10000$, $Q = 1.3$: 1 – $\vartheta = 0°$, 2 – $\vartheta = 90°$, 3 – $\vartheta = 180°$ (U_0, f_0 – averaged values of the velocity and the scalar at the mixer axis).

The internal flow asymmetry was also observed due to a sharp divergence of the square channel [13]. Asymmetric recirculation zones were generated just behind the place of channel divergence when the issuing flow transited from a laminar to a turbulent regime. This flow model is very similar to the one for the *r*-mode mixing regime, where the jet-to-co-flow velocity ratio is $U_d/U_D \sim 20$. It seems that at large Reynolds numbers, among the reasons for the asymmetry of the flow is its perturbations initiated by the inaccuracy of the mixer geometry.

We presented the experimental distributions at that angular position of the nozzle, at which the deviations of flow parameters from the symmetry were minimal.

The backflow was realized in a thin layer near the mixer wall and was registered through changing the sign of the averaged velocity profile in the mixer cross-section only at $x/D = 2.6$, shown in Fig. 3(a). It was thus impossible from the velocity profiles to establish the recirculation zone boundaries but only those, at which the flow structure changed at $x/D > 3.1$. For the *r*-mode mixing regime but with somewhat different parameters $Q = 1.02$, $D/d = 13.5$, the backflow range was within $0.4 \leqslant x/D \leqslant 3.0$ behind the nozzle [6]. Barchilon and Curtet [6] also established that increasing the parameter Q is accompanied by displacing the front boundary and the center of the recirculation zone downstream, while the boundary of its decay remains invariable near the cross-section at $x/D = 3.0$.

In the present study, the level of turbulent fluctuations increased over the mixer cross-section downstream of the nozzle, showing how the recirculation zone had developed. This was consistent with the dynamics of fluctuations [6]. The large fluctuations of the velocity near the wall at $x/D = 5.1$ reflect that this cross-section is near the back boundary of the recirculation zone where the flow is separated from the mixer walls. In Fig. 3(b), the velocity fluctuations behind this cross-section quickly decreased with developing uniform distributions across the mixer. In comparison with the data [6], the results of Zhdanov et al. [14] are evident of the fact that the observed difference in the recirculation zone length depends on the diameter ratio D/d.

In Fig. 3(c), the scalar distributions indicate that the backflow occurs over the mixer cross-section already at $x/D = 0.6$. Downstream of the nozzle, the averaged scalar profiles are broadened more rapidly as against the averaged velocity ones. As a result, the quasi-homogeneous composition of mixture is seen over the mixer cross-section already at the distance $x/D = 5.1$ and is set prior to a formed uniform velocity distribution ($x/D > 9.1$). A faster spreading of the scalar profile along the mixer axis reveals the role of unsteady vortices of the jet in transport of passive admixture. As the Schmidt number for a considered medium is very large ($Sc > 1000$), i.e., diffusive transfer of the scalar is unessential as against convective one, a high intermittence level at the jet boundary predetermines the

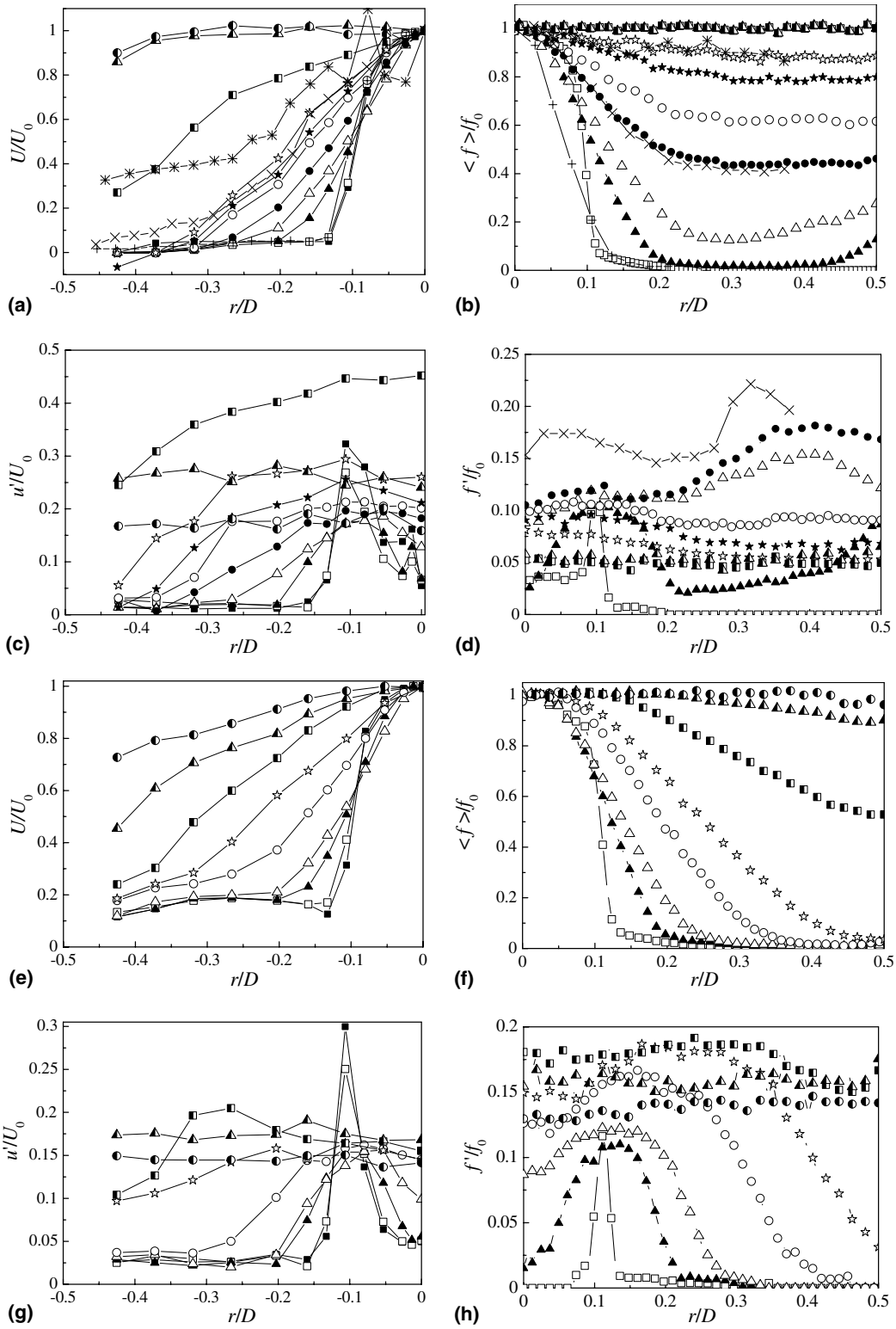

Fig. 3. Radial distributions of the averaged values of the longitudinal velocity component (a; e), the scalar (b; f) and root-mean-square fluctuations of these quantities (c, d; g, h) for $Re_d = 10000$ ((a)–(d) – $Q = 1.3$; (e)–(h) – $Q = 5$) at different distances from the nozzle: –■– $x/D = 0$, –□– 0.1, –▲–0.6, –△– 1.1, –●– 1.6, –○– 2.1, –★– 2.6, –☆– 3.1, –◧– 5.1, –◐– 7.1, –◭– 9.1; experimental data of Guiraud et al. [7]: (+) – $x/D = 0.1$, (×) – 1.74, (∗) – 3.14.

size of the region occupied by the scalar. The intermittence is related to unsteady vortex structures of the shear layer, whose size increases downstream. The field of time-averaged velocity points to the most probable position of the jet boundary, in fact neglecting the unsteady motion of the jet that manifests itself in scalar distributions.

The distinctive feature of the backflow is its unsteady behaviour. In spite of the fact that velocity fluctuations are quite small near the wall in the recirculation zone, the scalar fluctuations are high and wide ($x/D = 1.1, 1.6$). As the averaged backflow occupies a much narrower region near the wall in comparison with that of maximum scalar fluctuations, the latter are the result of backflow oscillations. Another support of this conclusion follows from the analysis of the behaviour of the scalar and its fluctuations. It is obvious that the scalar fluctuations are maximal at the boundary, at which the backflow carrying passive admixture interacts with the co-flow. The maximum scalar gradient near the mixer walls is in the cross-section at $x/D \sim 0.6$ and gradually decreases downstream, shown in Fig. 3(c). But the level of large scalar fluctuations in the wall region ($r/D > 0.4$, $x/D = 0.6$) remains invariable downstream up to the coordinate $r/D > 0.3$ ($1.1 \leqslant x/D \leqslant 1.6$) and then starts decreasing. So, the only reason for this level of large fluctuations is the oscillation of the backflow. Since behind the cross-section at $x/D > 2.6$, the scalar gradient across the mixer is small, the influence of backflow oscillations on the scalar fluctuations decreases. Proceeding from these concepts, it can be stated that the backflow is highly unsteady.

Some support to the quality of the data of the present study and the above conclusions on the unsteady behavior of the backflow can be found in Guiraud's investigation [7]. First of all, it should be noted that the mixer geometry in the both investigations is the same ($D/d = 5.0$) and the flowrate ratios are very close, $Q = 1.3$ in the present study and $Q = 1.44$ in Guiraud's work [7]. The velocity profiles over the first cross-section are really very similar in both studies but downstream [7], they drastically differ in faster spreading. As a result, the velocity profile at $x/D = 3.14$, obviously, characterizes the flow structure behind the recirculation zone, while at this very distance this zone still exists in our study as in work [6]. In Guiraud's work [7], the maximum velocity fluctuations in the jet shear layer monotonically increase up to $x/D = 3.14$, but in the present study, these are maximum in the first cross-section and then decrease with decreasing velocity gradient in the shear layer.

As shown in Guiraud's work [7], the scalar profiles are narrower than the velocity ones up to $x/D = 1.14$, while they should have at least the same width. At the same time, there is a good correlation between the scalar profiles at $x/D = 1.74$, 3.14 (see Ref. [7] in this article) and those at $x/D = 1.6$, 3.1 in the present study. In spite of the fact that the existence of the recirculation zone was not discussed [7], the distributions of scalar fluctuations at $x/D = 1.74$ clearly show the increase in their values near the mixer wall due to the backflow oscillation.

There are also some uncertainties in the velocity and scalar decay [7], shown in Fig. 4. The velocity fluctuations at the nozzle exit are quite small (about 5% of the averaged velocity) and cannot cause a sharp decrease in the scalar at the jet axis. This decrease in the scalar just behind the nozzle exit was observed by Zhdanov et al. [14] when the turbulence level at the nozzle exit was around 20%. From the data of the present study, it is seen that the jet starting length with a constant scalar exists and the scalar decay rate follows the averaged velocity one up to $x/D \sim 1.6$, shown in Fig. 4(b). It is clear that the scalar decay is determined by convective transfer and at least is equal to the velocity one. In the both discussed cases, the evolution of the scalar field is completed prior to that of the velocity one. At $x/D > 6$, the velocity and scalar values approach their asymptotic ones that can be found from the continuity condition $u = \frac{d^2}{D^2}(1+Q)$, $f = 1/(1+Q)$, assuming that perturbations due to the mixing nearly decay and the flow can be considered as a turbulent developed pipe flow. In the both investigations, the scalar fluctuations decay fast and do not change behind the distance $x/D = 5.1$.

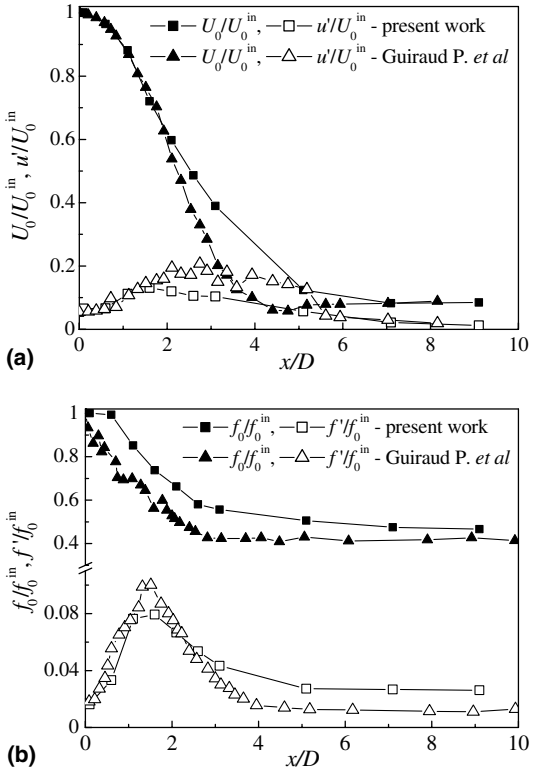

Fig. 4. Comparison of decay of velocity (a) and scalar (b) parameters in the *r*-mode regime from the present work and [7] (U_0^{in}, f_0^{in} – averaged values of the velocity and the scalar at the mixer axis near the nozzle exit).

j-mode mixing regime. This mixing regime is characterized both by a larger ratio of the co-flow velocity to the jet one and by a monotonic broadening of a velocity profile that reflects the development of the jet flow structure, as shown in Fig. 3(e)–(h). At $x/D < 2.1$, turbulent fluctuation profiles are essentially narrower and their maximum values are smaller than those in the *r*-mode regime due to the reduction of the velocity gradient across the shear layer. Despite of the fact that within the analyzed range $x/D < 9.1$, the averaged velocity distribution over the mixer cross-section is far from the uniform one, the turbulent fluctuation profiles in the cross-section at $x/D > 7.1$ are

quite uniform. Fluctuations values are lower than the corresponding ones for the identical cross-sections in the mixing regime with the recirculation zone, where the averaged velocity distribution is essentially more uniform.

The process of *j*-mode mixing occurs more slowly – a quasi-uniform scalar distribution starts developing only at $x/D = 9.1$. As in the *r*-mode mixing regime, the scalar profile becomes wider much more quickly than the velocity one obviously for the same reasons.

The profiles of the root-mean-square scalar fluctuations have wider maxima in comparison with the velocity ones and are broadened much more quickly than the first, reflecting the high level of intermittence in the jet shear layer. The values of scalar fluctuations over the cross-section at $x/D = 9.1$ are close to those of velocity ones and are almost three times larger as against those in the *r*-mode mixing regime.

The velocity and scalar decay along the mixer axis testifies that up to the cross-section at $x/D = 1.6$, the scalar evolution is determined through that of the averaged jet velocity, as shown in Fig. 5, i.e., the influence of the unsteady structures of the jet is still inconsiderable in virtue of their small scale. In the *j*-mode mixing regime, there is a little difference in the evolution of velocity and scalar fields downstream.

In the *r*-mode mixing regime, the averaged velocity behind the cross-section at $x/D = 1.6$ decays much more quickly than the scalar one. Turbulent fluctuations increase from the nozzle downstream, attain maximum values at $x/D = 5.1$ and quickly decay up to the cross-section at $x/D = 9.1$ where they approach the values determined in the *j*-mode regime. Scalar fluctuations also increase downstream, but only to the distance $x/D \sim 2$, then decrease and practically do not vary, starting with the cross-section at $x/D = 5.1$. As mentioned previously, they remain almost three times smaller than the scalar fluctuations in the *j*-mode mixing regime. This fact says that in the quasi-uniform state, a higher mixing degree is achieved when the recirculation zone is formed in the mixer.

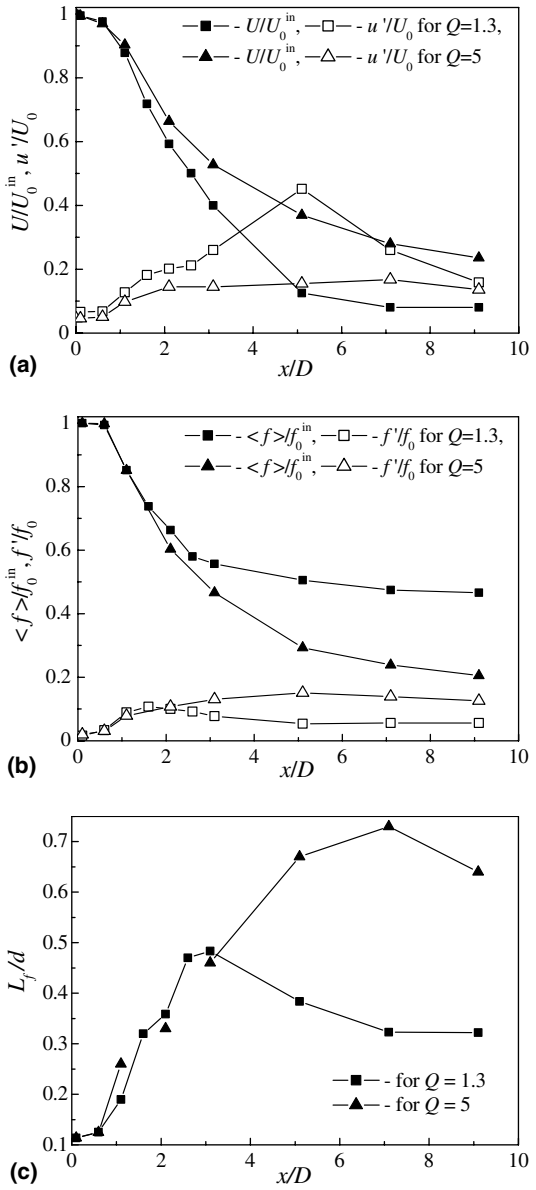

Fig. 5. Decay of the averaged values of the longitudinal velocity component, the averaged scalar and their root-mean-square fluctuations and variations of the integral length scale L_f along the mixer axis in different mixing regimes for $Re_d = 10000$.

3.2. Autocorrelation function and integral length scale of scalar fluctuations

Additional information on the scalar dynamics for the both mixing regimes can be obtained by analyzing the values of the transverse autocorrelation function calculated through the measured instantaneous scalar distributions $f(r)$:

$$R_f(r,\eta) = \frac{\langle f'(r) f'(r+\eta)\rangle}{\sqrt{\langle f'^2(r)\rangle}\sqrt{\langle f'^2(r+\eta)\rangle}}, \quad (1)$$

where $-0.5 < r/D < 0.5$.

Plots of autocorrelation function (1) at three points in the mixer cross-section are presented in Fig. 6. This provides grounds to follow the flow history at each of the points being analyzed. The autocorrelation function in the flow region, where the scalar value is close to constant and the fluctuations are small, is characterized by a narrow peak equal to unity. This situation is seen at each flow point in the first cross-section of the mixer.

For the *r*-mode mixing regime, this situation changes essentially already in the cross-section at $x/D = 0.6$. In Fig. 6(a), the domains of strong correlations develop near the mixer walls. It is clear that the existence of these domains is determined by large scalar fluctuations in the controlled region. The scalar has been brought by the backflow upstream of the co-flow to the cross-section. As shown previously, this averaged flow occupies a very small region near the wall at this distance from the nozzle. The only reason, which forces scalar fluctuations to spread in the region

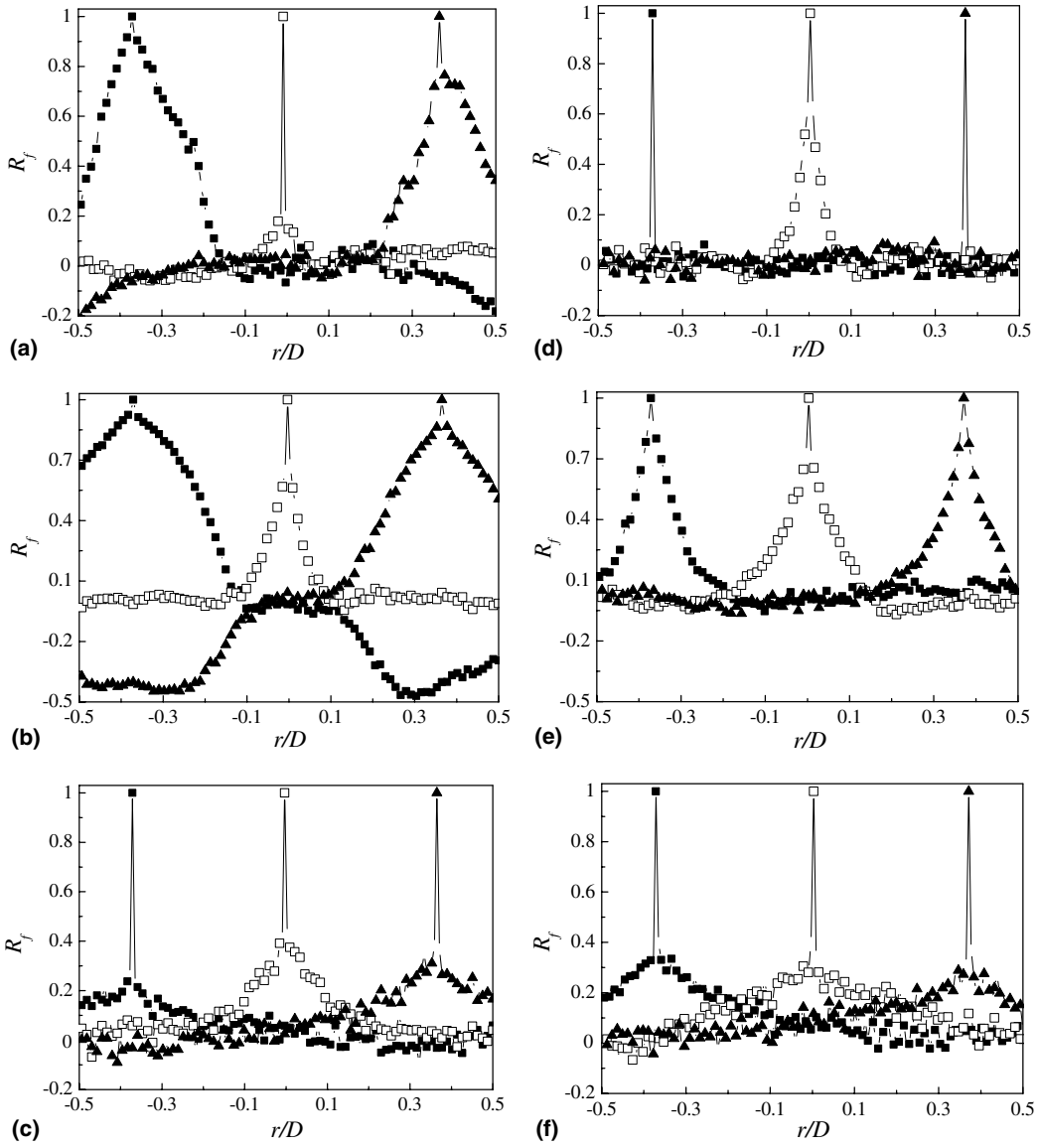

Fig. 6. Distributions of the autocorrelation function R_f for three points in the mixer cross-section (–■– $-r/D = 0.375$, –□– $-r/D = 0$, –▲– $-r/D = -0.375$) within two mixing regimes at different distances from the nozzle: (a) $x/D = 0.6$, (b) 1.6, (c) 3.1 for $Q = 1.3$; (d) $x/D = 1.1$, (e) 3.1, (f) 9.1 for $Q = 5$.

larger than the one occupied by the averaged backflow, is the oscillating character of the flow.

For each of the points $r/D = 0.375$ and -0.375, the correlations approach zero in the jet axis direction, but they again enhance, changing their sign for the negative one near the opposite wall. The changing of the correlation sign is a result of the phase shift of fluctuations across the jet mixer. The negative correlations are evident of the fact that the scalar and flow fluctuations near the opposite walls reveal the antiphase motion. Indeed, such a flow motion in the wall region is easily visualized. This agrees well with the instantaneous visualizations [6]. For the statistically averaged field, the phase shift is expected to be π and the minimum negative value attained by $R_f(r, \eta)$ is -1, whereas due to the flow axial asymmetry it is about -0.5.

A zero correlation between the points near the mixer wall and the point at the mixer axis means that the sources of scalar fluctuations in these regions are independent. The interaction of the jet vortex structures with the ones in the surrounding medium is very poor, therefore, the recirculation zone can be considered as two fluid regions with quite different characteristics.

Fig. 6(b) and (c) shows that the correlation domains near the mixer walls decrease downstream and fully decay at $x/D = 5.1$, indicating that the mixture is quasi-homogeneous. At the jet axis, the autocorrelation function changes monotonically and predictably, as shown in Fig. 6(a) and 6(c). Moving away from the nozzle, the area under the peak at the jet axis increases in size, because the scalar decreases and the scalar fluctuations increase as against

the initial ones due to the entrainment of the co-flow into the jet medium. In the region of the quasi-homogeneous mixture ($x/D \geqslant 5.1$), the autocorrelation function is again a narrow peak equal to unity.

In the *j*-mode mixing regime, the form of the autocorrelation function at the points $r/D = 0.375$ and -0.375 illustrates that the co-flow is not mixed with the jet up to the distance $x/D > 2.1$, as shown in Fig. 6(d). With the jet broadened, its vortex structures fill the entire mixer space, bringing the scalar to each point of the mixer cross-section and actually increasing the scalar fluctuations. This is seen in the development of the correlation domain near the mixer walls in the mixer cross-section at $x/D = 3.1$. Owing to the mixing, the scalar levels across the mixer and the scalar fluctuations decrease, causing the correlation domains to become narrower. At the distance $x/D = 9.1$, the autocorrelation function distributions over the mixer cross-section are fully identical to those over the cross-section at $x/D = 3.1$ in the *r*-mode mixing regime. Thus, it may be concluded that over the mixer cross-section at $x/D = 9.1$, the uniform scalar distribution has not been yet achieved and its completion should be expected downstream.

The transverse integral length scale of the scalar fluctuations over the mixer cross-section is calculated using the autocorrelation function R_f:

$$L_f(r) = \int_{-\infty}^{\infty} R_f(r,\eta)\mathrm{d}\eta. \tag{2}$$

Since this definition is strictly valid only for a homogeneous mixture, in Fig. 5(c) the values of the integral length scale are along the mixer axis, at which the mixture homogeneity is the highest.

For the both investigated mixing regimes, the values of the integral length scale at the mixer axis downstream of the nozzle first increase, revealing that the scalar vortex structures become larger. In the *r*-mode mixing regime, the integral length scale attains a maximum value of $L_f/d \sim 0.5$ over the cross-section at $x/D = 3.1$ and then gradually decreases, reflecting the degradation of large vortices. It is worth noticing that the integral length scale of the flow at the mixer periphery is larger than the one at the mixer axis, as shown in Fig. 6. Due to this fact, the mixing practically ends within the recirculation zone. But behind this zone ($x/D \geqslant 5.1$), the value of L_f becomes smaller. In the flow region at $x/D \geqslant 5.1$, where there exists the uniform scalar distribution across the mixer, the integral length scale attains a minimum value that remains almost constant across the mixer.

In the *j*-mode mixing regime, the integral length scale is maximum in value inside the shear layer and increases, attaining its largest value at the distance $x/D = 7.1$. The L_f variation along the mixer axis follows this tendency and the maximum value of $L_f/d \sim 0.7$ is attained at $x/D = 7.1$. A uniform length scale distribution is formed only in the central part of the mixer at $x/D = 9.1$. It is peculiar that in the both considered mixing regimes, the development of the integral length scale at the jet axis up to the mixer cross-section at $x/D = 3.1$ is very similar. Downstream this distance, the L_f variation is opposite: in the *r*-mode mixing regime, it decreases, while in the *j*-mode regime, it increases. The increasing of the integral length scale is obviously provided by a continuous growth of jet vortex structures, but its decreasing results from disintegrating the recirculation zone. Two quite independent flow regions of the recirculation zone begin to interact at $x/D \geqslant 3$ and this gives rise to the acceleration of decay of jet vortex structures. Figs. 3 and 5 illustrate that the behaviour of the turbulent fluctuations is obviously representative of these processes.

3.3. Structure of the recirculation zone

The above data of the analysis of the mixing development in the recirculation zone reveal the flow features that have not been discussed previously in the available literature. These features are: (1) existence of two different types of the flow in the recirculation region; (2) oscillating backflow fluid, i.e., averaged unsteady flow; (3) fluid oscillating in the antiphase near the opposite walls; (4) flow asymmetry.

In Fig. 7, the radial distributions of the Reynolds-averaged flowrate enables identifying the recirculation zone as a surface governed by the constant stream-function $\Psi/\dot{V}_d = 1 + Q$. As seen, the recirculation zone is located

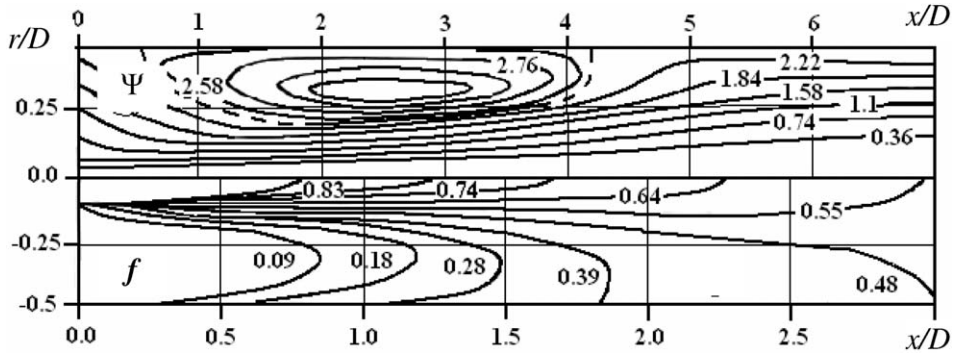

Fig. 7. Streamlines (top) and mixture fraction isolines (bottom) in the jet mixer for $Re_d = 10000$, $Q = 1.3$.

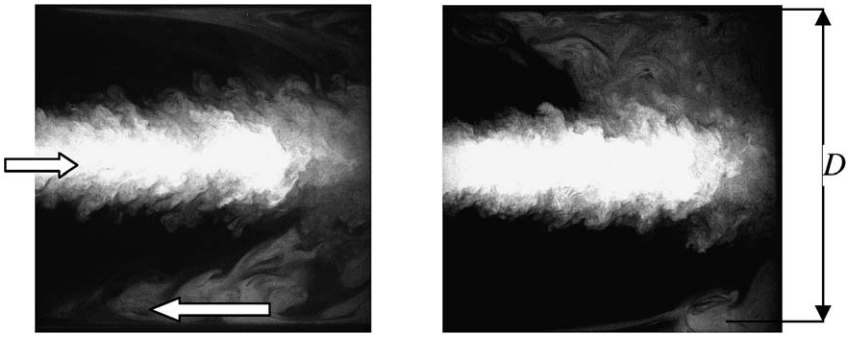

Fig. 8. Instantaneous flow patterns of the scalar field in the r-mode mixing regime ($Q = 1.3$) with a 1 s interval.

behind the nozzle in the range $0.5 < x/D < 4.2$. This model of a three-dimensional steady vortex created in the recirculation zone was first proposed by Batchilon and Curter [6]. In this work, for the somewhat different mixer geometry ($D/d = 13.5$), but for the nearly same mixing regime ($Q = 1.02$), this range was $0.4 \leqslant x/D \leqslant 3$. As seen from the bottom of the flow pattern, the most intense mixing processes occur in the front part of the recirculation zone within $0.5 < x/D \leqslant 2.0$, whereas the mixing state is close to the homogeneous one in the back part at $x/D > 3$.

The representation of the recirculation zone given by the authors [6] differs considerably from the instantaneous flow pattern visualized by the LIF method, as shown in Fig. 8, and cannot explain the above data on velocity and scalar fields.

In reality, the recirculation zone is a cluster of unsteady vortices. The backflow, carrying the scalar, moves along the mixer wall in the direction opposite to the co-flow and is very thin in the cross-section just behind the nozzle. The 17 s video film shows that the opposite passive admixture layers oscillate along the mixer walls in the antiphase with a period of ~5 s. In Fig. 9, these long-period oscillations are clearly seen from the time series of the mixture fraction recorded for two symmetric points $r/D = \pm 0.25$ at $x/D = 1.6$. As a result of these oscillations, the scalar fluctuations are large in the wall layer when $x/D > 0.6$, shown in Fig. 3(b).

The oscillation period T_c can also be estimated as the ratio of the characteristic scale L_c to the velocity, V_c, of the cluster of vortices. In Fig. 7, the center of the recirculation zone is located at $r/D = 0.35$. The averaged velocity at $r/D = 0.35$ is $V_c \approx 0.022$ m/s. Taking L_c approximately equal to $3D$, we obtain a rough estimation of the oscillation period $T_c = L_c/V_c \approx 6.8$ s. In Fig. 10, the dominant modes of oscillations are seen in the spectra of mixture fraction fluctuations averaged over four different measurements. These modes have a period of about $100/15 \approx 6.7$ s at $r/D = 0.125$, 0.25 and of about 6 s at $r/D = -0.25$, which is in agreement with the time series of the signal, as shown in Fig. 9, and the rough estimation of T_c. The

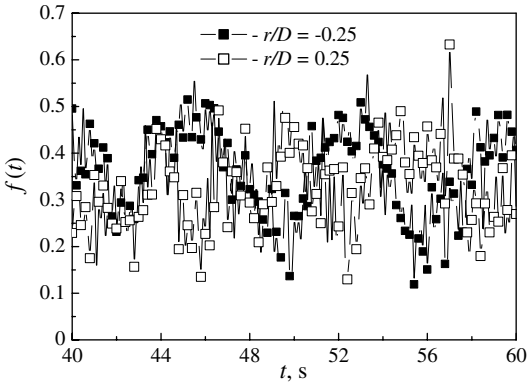

Fig. 9. Time series of the mixture fraction at $x/D = 1.6$ in the r-mode mixing regime ($Q = 1.3$).

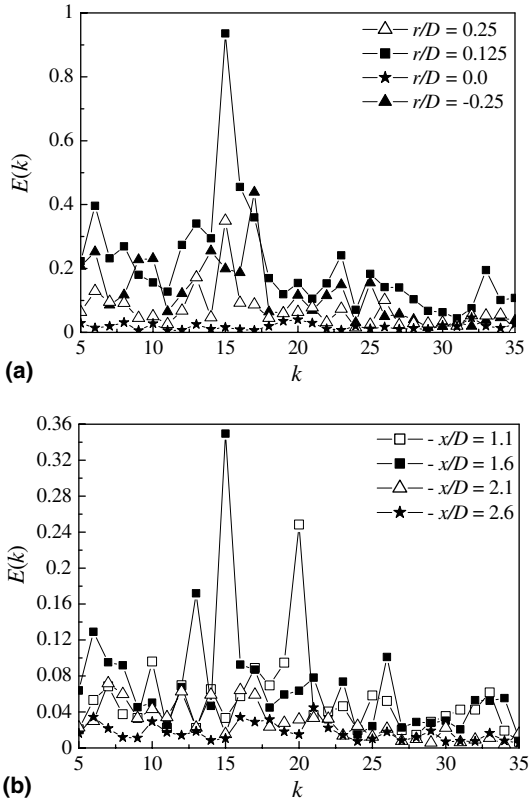

Fig. 10. Scalar fluctuation spectra in the r-mode mixing regime: (a) at $x/D = 1.6$, (b) at $r/D = 0.25$.

Strouhal number based on the tube diameter $D = 0.05$ m and the incoming co-flow velocity $U_D = 0.063$ m/s is $Sh = D/U_D T_c = 0.12$.

The spectrum of the scalar fluctuations with a dominant frequency is typical only for some part of the recirculation zone. Figs. 10 and 11 illustrate that the dominant modes disappear in the region full of small-scale vortices at $x/D \geqslant 2$ and near the mixer axis.

Fig. 11(a) and (b) shows that the inertial convective subrange of the spectrum of scalar fluctuations can be observed in some part of the recirculation zone. As known, the power law for this spectrum subrange depends on turbulent Reynolds and Schmidt numbers. When $Re_\lambda \gg 1$ and $Sc \gg 1$, $E(k) \approx k^{-5/3}$ is valid but for the smaller Re_λ, the power decreases up to -1.42 or -1 (see Ref. [15] in this article). The inertial convective subrange being observed at rather low wave numbers points to large scales of the structures peculiar of this subrange. Another conclusion that can be done from spectrum distributions is concerned with the homogeneity of the recirculation zone. It is clear that the zone structure changes essentially along and across it. In Fig. 11(c), the inertial convective subrange is not yet resolved at the mixer axis. In the *j*-mode mixing regime, the flow structure is rather simple and trivial, no oscillations are observed.

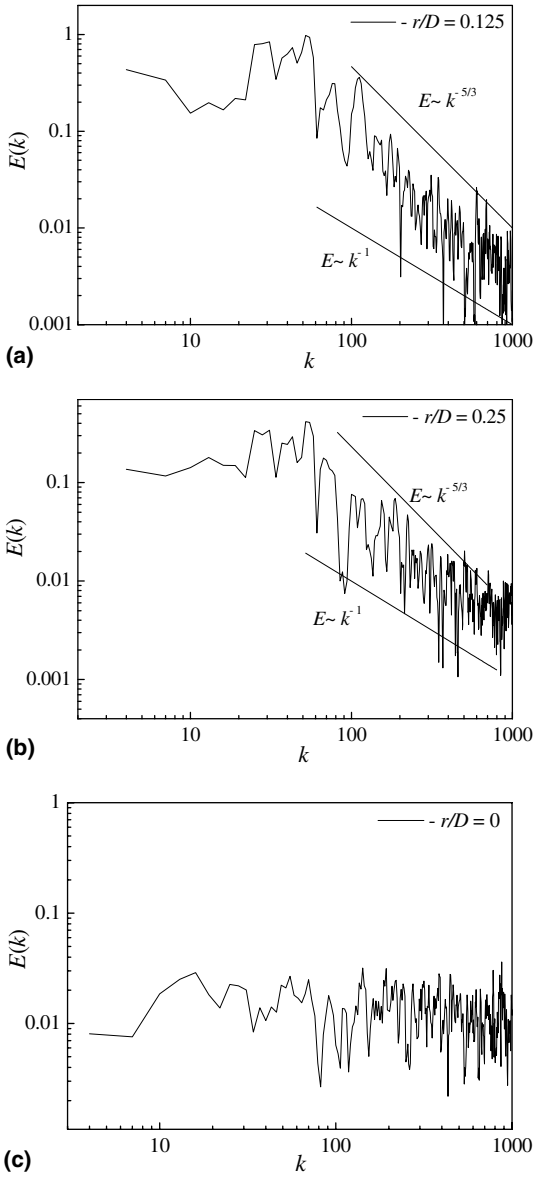

Fig. 11. Scalar fluctuation spectra at $x/D = 1.1$ in the *r*-mode mixing regime ($Q = 1.3$).

The presence of long-period oscillations in the recirculation zone has a strong impact on the methodology of CFD assessment if the mixing is being calculated in the jet mixer. A simulation time should be so long as to resolve these oscillations. Besides classical Reynolds-averaged quantities, the period and amplitude of oscillations are of importance for validation. The resolution should be so high that vortex structures could be reliably described in the jet flow, as well as in the recirculation zone.

3.4. PDF analysis of the scalar field

According to the definitions [16], the mixing stages in different jet mixer cross-sections can be classified as follows: macromixing – poorly macromixed and poorly micromixed (radial coordinate-dependent f); mesomixing – well macromixed and poorly micromixed ($f(x,r) = \text{const}$) over the entire cross-section and scalar fluctuations f' are not zero ($f' \neq 0$); micromixing – well macromixed and well micromixed ($f(x,r) = \text{const}$) over the entire cross-section and scalar fluctuations f' are zero ($f' = 0$). The mixing stage, at which the scalar distribution is uniform across the mixer, is quite easy to fix. For the *r*-mode mixing regime, this stage is reached already at $x/D = 5.1$. The scalar fluctuations are not equal to zero even over the cross-section at $x/D = 9.1$, but they do not change, already starting with the distance $x/D > 5.1$. The zero level of scalar fluctuations could not be measured because of electronic equipment noise. Due to this fact, it is not easy to determine, how far the actual mixture state is from the micromixing one.

The attainment of the micromixing state can be judged through the one-point scalar PDF, serving as a good criterion for fine-grained mixing bound up with the interaction of small-scale turbulent motions and molecular diffusion in the flow. Unlike the statistical moments (averaged scalar and root-mean-square fluctuations responsible for the integral properties of the scalar field), such a function contains the probabilistic information on all the values of the scalar that can be at a given flow point.

The scalar PDF for a homogeneous mixture is characterized by the δ-function, while that for a quasi-homogeneous one – by a Gaussian distribution. The scalar PDF is determined from the experimental instantaneous mixture fraction distributions as

$$P_{\exp}(f) = \lim_{N\to\infty} [N_m(f)/(Nh)]. \quad (3)$$

This experimentally found function was compared with the predicted scalar PDF in the form of the β-distribution [16]:

$$P(f) = \frac{f^{\alpha-1}(1-f)^{\beta-1}}{\int_0^1 f^{\alpha-1}(1-f)^{\beta-1}\mathrm{d}f}. \quad (4)$$

In (4), two positive parameters α, β are connected with the averaged value of the scalar $\langle f\rangle = \int_0^1 fP(f)\mathrm{d}f$ and the scalar variance $f'^2 = \int_0^1 (f-\langle f\rangle)^2 P(f)\mathrm{d}f$ by the relations [16]:

$$\alpha = \langle f\rangle[\langle f\rangle(1-\langle f\rangle)/f'^2 - 1], \quad \beta = \alpha(1-\langle f\rangle)/\langle f\rangle.$$

The statistical moments of higher order: skewness Sk and flatness T are related to the intermittence phenomenon induced by a wide spectrum of the existing length scales throughout the flow field. Moreover, in order to directly gain the information on the profile of the scalar PDF, it is possible to consider Sk and T determined from the experimental data as:

$$Sk = \frac{1}{N}\sum_{n=1}^{N}\left(\frac{f_n - \langle f\rangle}{f'}\right)^3, \quad T = \frac{1}{N}\sum_{n=1}^{N}\left(\frac{f_n - \langle f\rangle}{f'}\right)^4. \quad (5)$$

The skewness is responsible for the displacement degree of the scalar PDF profile with respect to the averaged value of the mixture fraction $\langle f\rangle$, while the flatness points to the slope degree of this function as against its Gaussian form:

$$P_G(f) = \frac{1}{\sqrt{2\pi f'^2}}\exp\left\{-\frac{(f-\langle f\rangle)^2}{2f'^2}\right\}. \quad (6)$$

The Gaussian PDF is indicative of the asymptotic mixed state of the medium. It is a symmetrical one, therefore, $Sk = 0$ and $T = 3$.

In the both regimes the PDF on the mixer axis (Fig. 12) has a steep one-mode profile that is narrowed downstream. The PDF form differs essentially from the δ-function at the distance $x/D = 7.1$, and a relatively high level of scalar fluctuations (Fig. 3(d) and (h)) is evident of the fact that the micromixing remains unfinished for the both considered mixing regimes. Fig. 12 also shows that β-distribution (4) can be used as a theoretical model that governs experimental PDFs in the computational domain near the axis.

The behaviour of the scalar PDF over the mixer cross-section is analysed with the use of skewness and flatness. These statistical moments depicted in Fig. 13 are calculated using both the scalar PDF determined from the experimental scalar realizations and the β-distribution, relation (4). In the r-mode mixing regime, two large-intermittence regions of the scalar field develop just behind the nozzle. The positive maximum of the skewness reflects that the probability of small scalar values is very high, i.e., the PDF profile is elongated in the direction of the large scalar, which is peculiar of the wall flow. The negative skewness at the jet axis is caused by the medium of the co-flow entrained into the jet, and the concentration of the initially homogeneous admixture decreases. In Fig. 13(a), unlike the large intermittence near the mixer walls, the one observed at the jet axis weakly shows up over the mixer cross-section at $x/D = 0.6$. The intermittence rapidly decays downstream, but the regions with the different-sign skewness remain up to the distance $x/D = 1.6$.

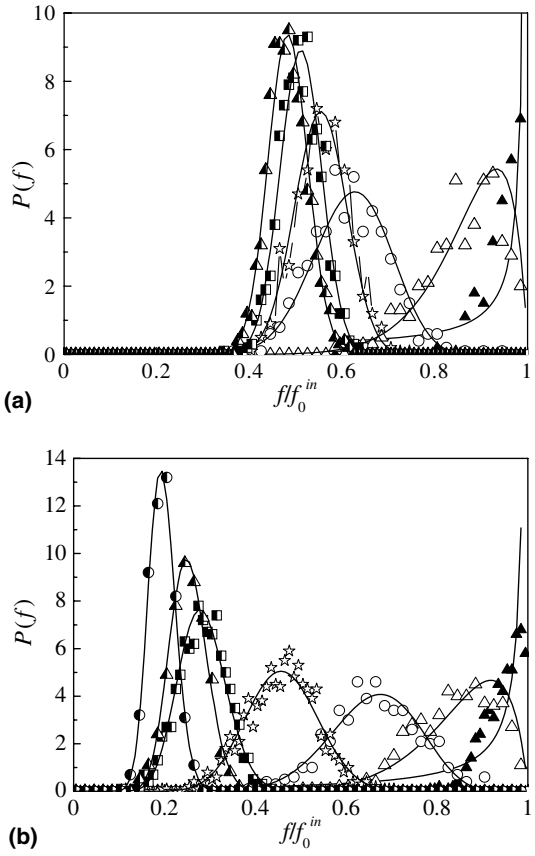

Fig. 12. Scalar PDF (3) calculated in terms of the experimental scalar values versus theoretical scalar PDF in the form of β-distribution (4) along the mixer axis at different distances from the nozzle: symbols – experimental scalar PDF (see the notations in Fig. 3), lines – theoretical scalar PDF.

In the large-intermittence region, the values of the skewness and flatness, peculiar of the β-distribution, do not agree with those calculated from the experimental data. However, in the mixer cross-section at $x/D = 1.1$ a qualitative agreement is seen between them.

At the distance $x/D = 1.6$, the experimental skewness distribution is a mirror reflection with respect to the same distribution found using the scalar PDF in the form of the β-distribution. The flatness values show that unlike the theoretical scalar PDF, the experimental one differs essentially from the Gaussian distribution. It should be noted that the disadvantage of a priori assignment of the form of the scalar PDF, which was determined using only first two statistical moments of the scalar field – averaged value of the scalar and its root-mean-square fluctuations, is most clearly seen by the example of the Sk and T distributions over the cross-section at $x/D = 1.6$. Indeed, the available data shown in Fig. 14 and the numerous

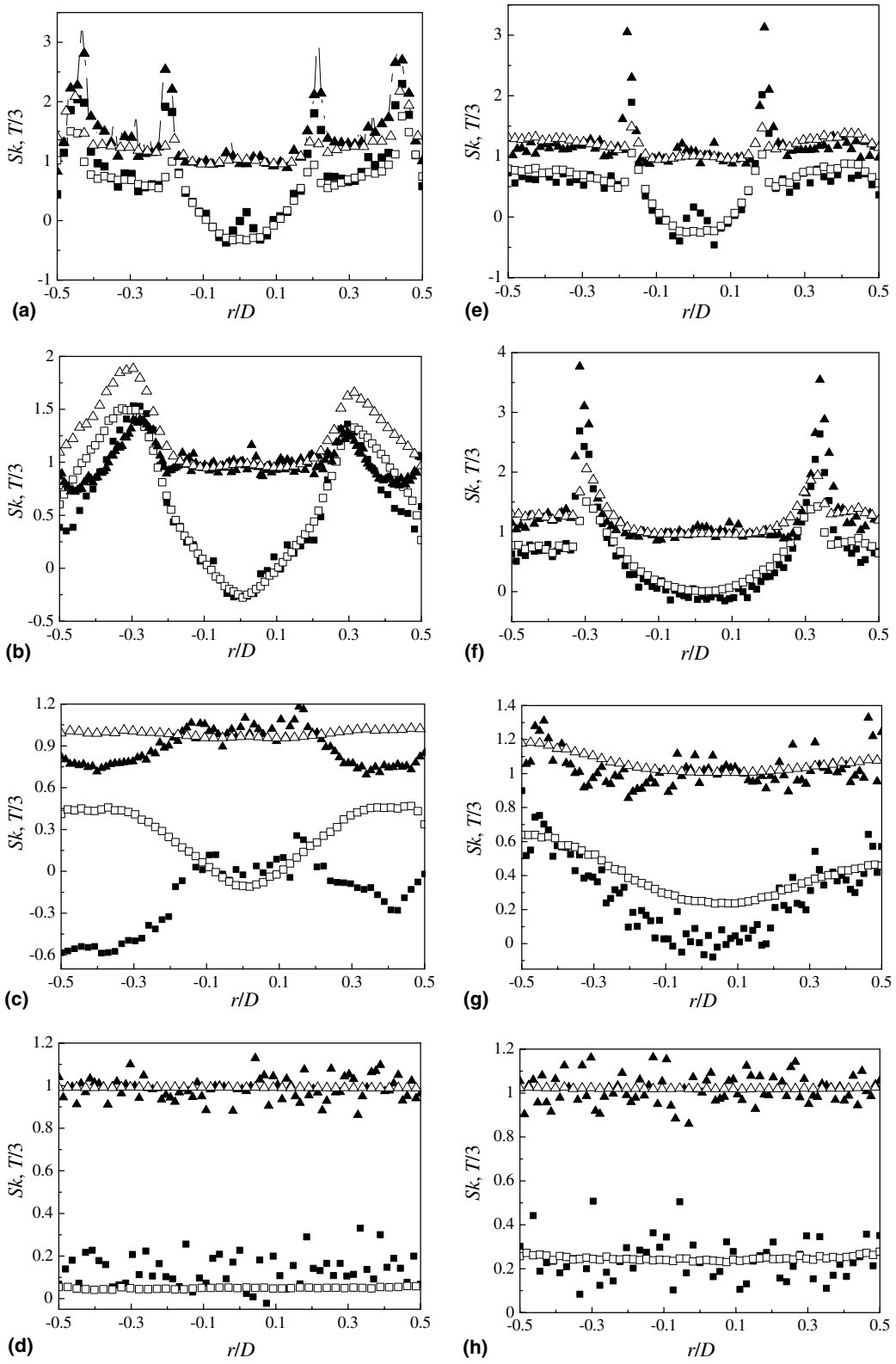

Fig. 13. Distributions of skewness and flatness over the mixer cross-section within two mixing regimes : (a) $x/D = 0.6$, (b) 1.1, (c) 1.6, (d) 5.1 for $Q = 1.3$; (e) $x/D = 0.6$, (f) 2.1, (g) 5.1, (h) 9.1 for $Q = 5$ (■, ▲ – experimental values of Sk and $T/3$; □, △) – the same parameters calculated by the theoretical scalar PDF in the form of β-distribution (4).

experimental results illustrate that at different flow points there can appear a much more complex (e.g., bimodal) form of the PDF, whose two-parameter representation does not hold true [16].

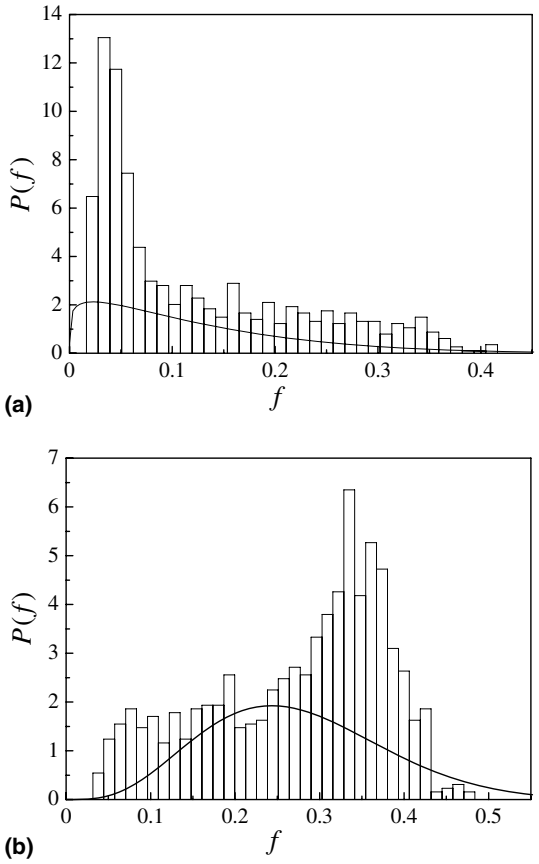

Fig. 14. Scalar PDF for a point of the recirculation zone with the coordinates $r/D = 0.12$: (a) $x/D = 1.1$; (b) $x/D = 1.6$ (lines – theoretical scalar PDF in the form of β-distribution (4), columns – experimental scalar PDF).

As follows from the probability theory, ascertaining that the information on statistical moments of all orders is equivalent to the one accumulated in the distribution function, it is necessary to use a larger number of statistical moments for the scalar PDF being reconstructed. One of the methods developed within the framework of statistical physics is a procedure of reconstructing the scalar PDF based on the hypothesis that the predicted form of this function must provide maximum statistical entropy and be consistent with the information on the known moments of the corresponding random fields [17].

The flatness value of the considered scalar PDF agrees with that characteristic for the Gaussian distribution in the region of the scalar homogeneous state ($x/D = 5.1$). However, the skewness values different from zero testify that different mixing length scales are present, i.e., the micromixing process is not completed. In this case, it is evident from Fig. 13(d) that the Sk values determined from the β-distribution of the scalar PDF misrepresent the real information on the micromixing rate.

As for the j-mode mixing regime, the use of the β-distribution for the scalar PDF as the model that adequately describes the real mixing processes is beyond question, shown in Fig. 13(e) and (f). Some of the problems on fitting the β-distribution to the experimental scalar PDF remain in the narrow region of intermittence at the jet boundary. The possibility of using the β-distribution to describe the scalar PDF has been emphasized [10].

4. Conclusions

This experimental study of two mixing regimes in the coaxial jet mixer has revealed an essential difference in the development of velocity and scalar fields. Over the investigated distance range $0.1 \leqslant x/D \leqslant 9.1$, the uniform averaged velocity field has no time to form, although when the recirculation zone is formed, the uniform averaged velocity distribution is set along the larger part of the mixer cross-section.

In the r-mode mixing regime, the formation of a quasi-uniform scalar field is completed up to the mixer cross-section at $x/D = 5.1$, whereas in the j-mode mixing regime, this process at $x/D = 9.1$ only reaches the stage of its completion. In the r-mode mixing regime, the level of scalar fluctuations in quasi-homogeneous mixture is about three times smaller.

Thus, the scalar field develops ahead the velocity one. Since scalar transfer is determined by the flow dynamics, a more rapid development of the jet scalar field can be attributed to the influence of unsteady vortex structures generated in the mixing layer during scalar transfer. These vortex structures provide scalar transfer across the mixer at larger distances behind the statistically determined jet boundary.

Based on the present study, a new standpoint of the recirculation zone has been stated. Analysis of the scalar fluctuation spectrum and the autocorrelation function shows that behind the nozzle, there are two different weakly interacting flow regions: jet and surrounding medium initiated by interaction between the backflow and co-flow. Long-period asymmetric oscillations of the backflow were fixed from both the analysis of the turbulent statistic characteristics and flow visualizations. There are the flow regions within the recirculation zone where the inertial convective sub-range in the scalar fluctuation spectrum exists. So, this zone is a superposition of unsteady vortices of different length and time scales. Its representation as a three-dimensional steady vortex [6] is not adequate to the flow nature. Evidently, theoretical models used to calculate the mixing should account for the existence of different length scales in the recirculation zone and a strong unsteady behavior of the flow. One of the most appropriate candidates for this is large Eddy simulation (LES).

Analysis of the scalar PDFs and also of the skewness and flatness distributions is beneficial in the estimation of the actual mixture state, how far it is from that of complete mixing. For the both examined regimes, the micromixing process over the investigated distance range does not end. The use of the scalar PDF in the form of the β-distribution for scalar field calculations testifies that this function differs

considerably from the experimental one in the large-intermittence region. Here, not only great quantitative discrepancies in the predicted and experimental values of the skewness and flatness exist but also their qualitatively different behavior is observed. Also, the considered β-approximation of the scalar PDF yields that the end of the micromixing process is somewhat overestimated.

Acknowledgements

The study has been supported by Deutsche Forschungsgemeinschaft within the framework of the Program SPPP 1141 and Belarusian Republican Foundation of Fundamental Research within the framework of the Project T06MC-042.

References

[1] H. Rehalb, E. Villermaux, E.J. Hopfeinger, Flow regimes of large-velocity-ratio coaxial jets, J. Fluid Mech. 345 (1997) 357–381.
[2] E. Villermaux, H. Rehalb, Mixing in coaxial jets, J. Fluid Mech. 425 (2000) 161–185.
[3] M. Lima, J. Palma, Mixing in coaxial confined jets of large velocity ratio, in: Proc. 10th Int. Symp. on Application of laser technique in fluid mechanics, 2002, Lisboa, 8–11 July.
[4] H.J. Henzler, Investigations on mixing fluids. Ph.D. thesis, 1978, Aachen, RWTH.
[5] K.H. Tebel, H.O. May, Der Freistrahlreaktor – Ein effektives Reaktordesign zur Unterdrueckung von Selektivitaetsverlusten durch schnelle, unerwünschte Folgereaktionen, Chem. Ing. Tech. 60: (11) (1988) 1708–1788.
[6] M. Barchilon, R. Curtet, Some details of the structure of an axis-symmetrical confined jet with backflow, J. Basic Eng. Dec. (1964) 777–787.
[7] P. Guiraud, J. Bertrand, J. Costes, Laser Measurements of local velocity and concentration in a turbulent jet-stirred tubular reactor, Chem. Eng. Sci. 46 (5/6) (1991) 1289–1297.
[8] V.L. Zhdanov, N.V. Kornev, and E. Hassel, LIF investigation of the concentration field in the coaxial mixer. Lasermethoden in der Strömungsmesstechnik, 12 Fachtagung, 7–9 September, 2004. Karlsruhe: Universität Karlsruhe, 2004, pp. 16-1–16-8.
[9] V.L. Zhdanov, A.D. Chorny, N.V. Kornev, E. Hassel, Formation of a passive admixture concentration field in the coaxial mixer, Doklady Nat. Acad. Sci., Belarus 75 (4) (2005) 125–129.
[10] M. Mortensen, W. Orciuch, M. Bouaifi, B. Andersson, Mixing of a jet in a pipe, Chem. Eng. Res. Des. (2004) 357–363.
[11] J. Baldyga, J. Bourne, Turbulent Mixing and Chemical Reactions, Wiley and Sons, 1999.
[12] A. Roshko, On the drag and shedding frequency of two-dimensional bluff bodies, NACA Technical Note 3169 (1954).
[13] Y. Salhi, M. Hammoudi, E.K. Si Ahmed, F. Aloui, M. Souhar, On the velocity and pressure fields of a turbulent asymmetric flow with sudden expansion, in: Proc. of HEFAT 2005: 4th Int. Conf. Heat Transfer, Fluid Mechanics and Thermodynamics, Cairo, Egypt, 2005, 19–22 September, SY1.
[14] V.L. Zhdanov, N.V. Kornev, and E. Hassel, The influence of the mixer geometry on the scalar field formation. Lasermethoden in der Strömungsmesstechnik, 13 Fachtagung, 6–8 September, 2005. Cottbus, Germany, pp. 37-1–37-8.
[15] G. Brethouwer, Mixing of passive and reactive scalars in turbulent flow. A numerical study. Ph.D. thesis, 2001, Delft.
[16] R. Fox, Computational models for turbulent reacting flows, Cambridge University Press, Cambridge, 2003.
[17] S.B. Pope, A rational method of determining probability distributions in turbulent reacting flows, J. Non-Equilib. Thermodyn. 4 (1979) 309–320.